2018 European Control Conference (ECC)
June 12-15, 2018. Limassol, Cyprus

A Consensus-Based Control Law for Accurate Frequency Restoration and Power Sharing in Microgrids in the Presence of Clock Drifts*

Ajay Krishna[1], Johannes Schiffer[2] and Jörg Raisch[1,3]

***Abstract*— Clock drifts are a common phenomenon in distributed systems, such as microgrids (MGs). Unfortunately, if not accounted for, the presence of clock drifts can hamper accurate frequency restoration and power sharing in MGs. As a consequence, we have proposed in [1] a distributed secondary frequency control that ensures an accurate stationary control performance in the presence of clock drifts. In the present work, we extend the analysis in [1] by providing a tuning criterion for the controller parameters that guarantees robust stability of a given equilibrium point of the closed-loop dynamics with respect to uncertain bounded clock drifts. Finally, our analysis is validated via simulation.**

I. Introduction

Electric power systems around the globe are currently facing new changes and challenges which are mainly due to the increasing presence of renewable energy sources (RESs). At present, the electric power system contains a large number of small units rather than a small number of large power stations. These small units are usually equipped with RESs. To interface RESs into the electric grid, power electronic inverters are used. The physical characteristics of inverters largely differ from the characteristics of conventional generators. Therefore, new and intelligent control concepts which ensure stable and reliable power system operation are needed. In this context, the concept of microgrids (MGs) is foreseen as a promising solution [2]. A MG is a locally controllable subset of a large power system. It consists of several RESs, storage units and corresponding loads. MGs can typically work in islanded or grid-tied mode [2]. In this paper, we are interested in the former case.

As in any AC power system, frequency stability is a key performance criterion in MGs. In inverter-dominated MGs, so-called grid forming inverters (GFIs) are employed for this task. A GFI is a voltage source inverter which is controlled using pre-defined voltage and frequency values [2], [3]. Inspired by conventional power systems, a hierarchical control strategy is advocated in case of MGs [4], out of which, in this paper, we are interested in *distributed secondary frequency control* [1], [5]–[9] which uses local information as well as neighboring information over a communication network to ensure frequency restoration and power sharing (PS).

*The project leading to this manuscript has received funding from the German Academic Exchange Service (DAAD) and the European Union's Horizon 2020 research and innovation programme under the Marie Skłodowska-Curie grant agreement No. 734832.

[1]Fachgebiet Regelungssysteme, Technische Universität Berlin, Germany. {krishna, raisch}@control.tu-berlin.de

[2]School of Electronic and Electrical Engineering, University of Leeds, UK. j.schiffer@leeds.ac.uk

[3]Max-Planck-Institut für Dynamik komplexer technischer Systeme, Magdeburg, Germany.

In an inverter-dominated MG, each inverter typically has only a local understanding of time, which leads to clock inaccuracies [10]. In practice, clock drifts [11], [12] are non-negligible phenomena in distributed MG control [1]. A main reason for this is that in the presence of clock drifts, the internal frequency of an inverter differs from its actual electrical frequency [10], [13]. However, in most of the work on distributed secondary frequency control, the effect of clock drifts is not considered and it is assumed that both the electrical and internal frequencies are identical. See for example, the *pinning control* scheme [5], or the distributed averaging integral (DAI) control [6]–[9]. In [1], we have shown that the presence of clock drifts impairs accurate frequency restoration and PS with the usual secondary control schemes. Recently, the deteriorating effect of clock drifts on secondary frequency control was reported also in [14]–[17].

As in sensor networks, time synchronization protocols [18], [19] could potentially be used to address clock drift issues. Yet, in the case of MGs, in order to implement these time synchronization protocols, an additional time synchronization control has to be designed and should typically be activated before the primary and secondary controllers. Adding such an additional control layer would increase the overall complexity of the hierarchical MG control architecture [4]. In [20], an angle droop control, with consensus based frequency and power control to ensure PS in the presence of clock drifts is proposed. Yet, the implementation of [20] requires complete knowledge of phase angles, which is often a restrictive assumption in practice. Furthermore, in the related works [14]–[17] neither conditions for stability nor conditions under which a given distributed frequency control scheme leads to accurate PS in the presence of clock drifts are provided.

Motivated by this, in [1], we have proposed an alternative secondary control law, termed generalized distributed averaging integral (GDAI) control, and provided a parametrization of the control parameters, such that the synchronized electrical frequency is the nominal frequency and, in addition, PS is ensured in the presence of clock drifts. Moreover, the GDAI control can be implemented without any additional time synchronization protocol. In this paper, we extend the work in [1] by providing a design criterion in the form of a set of linear matrix inequalities (LMIs) which ensures that the GDAI control renders asymptotic stability (AS) of the closed-loop equilibrium point in the presence of clock drifts and guarantees accurate frequency restoration and PS. Unlike in [20], we do not linearize the electrical network, instead we work with the non-linear MG model. Moreover, our design criterion does not require knowledge of the operating

point. We use a Lyapunov function with classic kinetic and potential energy terms to derive the design criterion [21], [22]. Finally, we illustrate via simulation that with our design criterion, the GDAI controller achieves accurate frequency restoration, PS and local AS.

The paper is organized as follows. In Section II, we recall some preliminaries of graph theory, introduce the MG model and the GDAI control. In Section III, the design criterion for the closed loop system in the presence of clock drifts is presented. In Section IV, the design criterion is solved numerically and the results are simulated for an exemplary MG. Finally, we summarize our work and suggest some future research directions in Section V.

II. Preliminaries

We denote by I_n the $n \times n$ identity matrix, by $\mathbb{0}_{n\times m}$ the $n \times m$ matrix with all entries equal to zero, by $\mathbb{1}_n$ the vector with all entries being equal to one and by $\mathbb{0}_n$ the zero vector. The maximum eigenvalue of a square symmetric matrix F is denoted by $\lambda_{\max}(F)$. The elements below the diagonal of F is denoted by $*$. If F is positive (negative) definite, we denote this by $F > 0$ ($F < 0$). If F is positive (negative) semidefinite, we denote this by $F \geq 0$ ($F \leq 0$). Moreover, $A > B$ means that $A - B > 0$. Let $x = \text{col}(x_i)$ denote a vector with entries x_i, $Y = \text{diag}(y_i)$ a diagonal matrix with diagonal entries y_i and $X = \text{blkdiag}(X_i)$ a block-diagonal matrix with block-diagonal matrix entries X_i.

A. Algebraic graph theory

A weighted undirected graph [23], [24] of order $n > 1$ is a triple $\mathcal{G} = (\mathcal{N}, \mathcal{E}, \mathcal{W})$ with set of vertices $\mathcal{N} = \{1, \dots, n\}$. Furthermore, $\mathcal{E} \subseteq [\mathcal{N}]^2$ is the set of edges, where $[\mathcal{N}]^2$ represents the set of all two-element subsets of $\mathcal{N}$ and $\mathcal{W} : \mathcal{E} \to \mathbb{R}_{>0}$ is a weight function. The entries of the adjacency matrix $\mathcal{A} \in \mathbb{R}^{n\times n}$ of $\mathcal{G}$ are $a_{ij} = a_{ji} = w_l > 0$ if $\{i, j\} \in \mathcal{E}$ where $w_l = w(i, j) = w(j, i)$ is the edge weight and $a_{ij} = a_{ji} = 0$ otherwise. The set of neighboring nodes of node i is given by $\mathcal{N}_i = \{j \in \mathcal{N} \,|\, a_{ij} \neq 0\}$. The diagonal degree matrix $\mathcal{D} \in \mathbb{R}^{n\times n}$ is given by $\mathcal{D} = \text{diag}\big(\sum_{j\in\mathcal{N}} a_{ij}\big)$. A path is an ordered sequence of nodes such that any pair of consecutive nodes in the sequence is connected by an edge. The graph $\mathcal{G}$ is called connected if there exists a path between every pair of distinct nodes. The Laplacian matrix $\mathcal{L} \in \mathbb{R}^{n\times n}$ of an undirected graph is given by $\mathcal{L} = \mathcal{D} - \mathcal{A}$. The Laplacian matrix $\mathcal{L}$ is symmetric and positive semi-definite. If and only if $\mathcal{G}$ is connected, $\mathcal{L}$ has a simple zero eigenvalue. Then, a corresponding right eigenvector is $\mathbb{1}_n$, i.e., $\mathcal{L}\mathbb{1}_n = \mathbb{0}_n$.

B. Primary-controlled MG model with clock drifts

We consider a Kron-reduced representation [25] of an inverter-based MG and denote its set of network nodes by $\mathcal{N} = \{1, ..., n\}$, $n > 1$. The phase angle and voltage magnitude at each bus $i \in \mathcal{N}$ are denoted by $\delta_i : \mathbb{R}_{\geq 0} \to \mathbb{R}$, respectively, $V_i : \mathbb{R}_{\geq 0} \to \mathbb{R}_{>0}$. The electrical frequency at the i-th node is denoted by $\omega_i = \dot{\delta}_i$. As customary in secondary frequency control design, we assume that all voltage amplitudes are constant and that the line admittances are purely inductive [7], [25]. The latter assumption is generally satisfied for MGs in which the inductive output impedance of the converter filter and/or transformer dominates the resistive part of the line impedances [26] and we only consider such MGs. Thus, if there is a power line between nodes $i \in \mathcal{N}$ and $k \in \mathcal{N}$, then this is represented by a nonzero susceptance $B_{ik} \in \mathbb{R}_{<0}$. Furthermore, the electrical network is assumed to be connected and the set of neighboring nodes of the i-th node is denoted by $\mathcal{N}_i = \{k \in \mathcal{N} \,|\, B_{ik} \neq 0\}$.

Following [10], [13], we denote by $\mu_i \in \mathbb{R}$ the constant relative drift of the clock of the i-th unit, $i \in \mathcal{N}$. In general, $|\mu_i| \ll 1$ is a small unknown parameter [10], [13]. Furthermore, it is convenient to introduce the *internal* frequency $\bar{\omega}_i : \mathbb{R}_{\geq 0} \to \mathbb{R}$ of the inverter at the i-th node which—under the assumption of sufficiently fast sampling times—yields the relation [10], [13] between the *internal* frequency $\bar{\omega}_i$ and the *electrical* frequency ω_i as $\bar{\omega}_i = (1 + \mu_i)\omega_i, \forall i \in \mathcal{N}$. In the sequel, we refer to $\mu_i \in \mathbb{R}$ as the clock drift factor or simply clock drift.

Following standard practice, we assume that all units are equipped with the usual primary frequency droop control [4]. Then the dynamics of the generation unit at the i-th node, $i \in \mathcal{N}$, is given by

$$\begin{aligned}(1 + \mu_i)\dot{\delta}_i &= (1 + \mu_i)\omega_i = \bar{\omega}_i,\\ (1 + \mu_i)M_i\dot{\bar{\omega}}_i &= -D_i(\bar{\omega}_i - \omega^d) + P_i^d - G_{ii}V_i^2 + u_i - P_i,\end{aligned} \tag{II.1}$$

where $\omega^d \in \mathbb{R}$ is the desired electrical frequency, $P_i^d \in \mathbb{R}$ is the desired active power set point, $G_{ii}V_i^2 \in \mathbb{R}_{\geq 0}$ represents the constant power load at the i-th node, $D_i \in \mathbb{R}_{>0}$ is the inverse droop coefficient and $M_i = \tau_{P_i} D_i$ is the virtual inertia coefficient, where $\tau_{P_i} \in \mathbb{R}_{>0}$ is the time constant of the low pass filter for the power measurement [27]. Furthermore, $u_i : \mathbb{R}_{\geq 0} \to \mathbb{R}$ is the secondary control input. The active power flow $P_i : \mathbb{R}^n \to \mathbb{R}$ at the i-th node is [25][1]

$$P_i = \sum\nolimits_{k\in\mathcal{N}_i} |B_{ik}|V_iV_k \sin(\delta_i - \delta_k). \tag{II.2}$$

To derive a compact model representation of the MG, it is convenient to introduce the matrices

$$\begin{aligned}&D = \text{diag}(D_i) \in \mathbb{R}_{>0}^{n\times n}, M = \text{diag}(M_i) \in \mathbb{R}_{>0}^{n\times n},\\ &\mu = \text{diag}(\mu_i) \in \mathbb{R}^{n\times n},\end{aligned}$$

and the vectors

$$\begin{aligned}&\delta = \text{col}(\delta_i) \in \mathbb{R}^n, \omega = \text{col}(\omega_i) \in \mathbb{R}^n, \bar{\omega} = \text{col}(\bar{\omega}_i) \in \mathbb{R}^n,\\ &P^{\text{net}} = \text{col}(P_i^d - G_{ii}V_i^2) \in \mathbb{R}^n, u = \text{col}(u_i) \in \mathbb{R}^n.\end{aligned}$$

Also, we introduce the *potential function* $U : \mathbb{R}^n \to \mathbb{R}$,

$$U(\delta) = -\sum\nolimits_{\{i,k\}\in[\mathcal{N}]^2} |B_{ik}|V_iV_k \cos(\delta_i - \delta_k).$$

Then, the dynamics (II.1), $\forall i \in \mathcal{N}$, can be written as

$$\begin{aligned}(I_n + \mu)\dot{\delta} &= \bar{\omega},\\ (I_n + \mu)M\dot{\bar{\omega}} &= -D(\bar{\omega} - \mathbb{1}_n\omega^d) + P^{\text{net}} + u - \nabla U(\delta),\end{aligned} \tag{II.3}$$

compactly. Observe that

$$\frac{dU(\delta)}{dt} = \nabla U^\top(\delta)\omega = \nabla U^\top(\delta)(I + \mu)^{-1}\bar{\omega},$$

and due to symmetry of the power flows P_i, $\mathbb{1}_n^\top \nabla U(\delta) = 0$.

[1]For notational simplicity, time arguments of all signals are omitted.

C. Generalized Averaging Integral Secondary control

In general, P^{net} in (II.3) is non-zero because the loads $G_{ii}V_i^2$ are usually unknown. Moreover, if the overall power balance is non-zero, then the steady state frequencies of the droop controlled MG (II.3) deviate from the nominal value ω^d. This steady state frequency error should be brought to zero using a secondary control law. In this paper, we focus on distributed secondary frequency control. Note that usually the internal frequency $\bar{\omega}_i$ is employed in distributed secondary frequency control [5], [6], [8], [9]. At first glance, this has the advantage that no additional frequency measurement is needed. However, it has been shown in [1] that the, generally unavoidable, presence of clock drifts also leads to non-negligible stationary frequency deviations when using any of the aforementioned control schemes. Motivated by this, we have proposed the following GDAI control in [1]

$$u = p, \quad (I_n + \mu)\dot{p} = -\left((\mathbf{B} + \mathbf{C}\mathcal{L}_C)(\bar{\omega} - \mathbb{1}_n\omega^d) + \mathbf{D}\mathcal{L}_C p\right), \tag{II.4}$$

where $\mathbf{B} \in \mathbb{R}^{n\times n}$, $\mathbf{C} \in \mathbb{R}^{n\times n}$ and $\mathbf{D} \in \mathbb{R}^{n\times n}_{>0}$ are diagonal controller matrices and $\mathcal{L}_\mathcal{C} \in \mathbb{R}^{n\times n}_{\geq 0}$ is the Laplacian matrix representing the communication network. For the subsequent analysis, it is convenient to introduce the notion below.

Definition 2.1: The closed loop system (II.3), (II.4) admits a synchronized motion if it has a solution for all $t \geq 0$ of the form

$$\delta^s(t) = \delta_0^s + \omega^s t, \quad \omega^s = \omega^* \mathbb{1}_n,$$

where $\omega^* \in \mathbb{R}$ is the synchronized electrical frequency and $\delta_0^s \in \mathbb{R}^n$ such that

$$|\delta_{0,i}^s - \delta_{0,k}^s| < \frac{\pi}{2} \quad \forall i \in \mathcal{N},\ \forall k \in \mathcal{N}_i.$$

The expression for ω^* is given by [1]

$$\omega^* = \frac{\mathbb{1}_n^T \mathbf{D}^{-1}\mathbf{B}\mathbb{1}_n}{\mathbb{1}_n^T \mathbf{D}^{-1}(\mathbf{B} + \mathbf{C}\mathcal{L}_\mathcal{C})(I_n + \mu)\mathbb{1}_n}\omega^d. \tag{II.5}$$

The matrix $\mathbf{B}$ is commonly called the *pinning gain matrix*, e.g. [5]. In the following, we define the clock of one of the units in the network as master clock, say the k-th unit, $k \geq 1$. Then, $\mu_k = 0$ and the drifts $\mu_i, i \neq k$ of all other clocks in the MG are expressed with respect to the master clock at k-th unit. In this scenario, it has been shown in [1] that selecting

$$\mathbf{B}\mu = \mathbb{0}_{n\times n}, \quad \mathbf{C} = -\mathbf{D}, \tag{II.6}$$

in (II.4) guarantees that $\omega^* = \omega^d$ in (II.5) together with active PS in the presence of clock drifts. Achieving both of these control objectives is, in general, not possible with [5] and the standard DAI control [6], [8], [9] in the presence of clock drifts, see [1] for more details.

D. Closed-Loop System

Combining (II.3) with (II.4) and using (II.6) yields the closed-loop dynamics

$$\begin{aligned}(I_n + \mu)\dot{\delta} &= \bar{\omega},\\ (I_n + \mu)M\dot{\bar{\omega}} &= -D(\bar{\omega} - \mathbb{1}_n\omega^d) - \nabla U(\delta) + P^{\text{net}} + p,\\ (I_n + \mu)\dot{p} &= -(\mathbf{B} - \mathbf{D}\mathcal{L}_C)(\bar{\omega} - \mathbb{1}_n\omega^d) - \mathbf{D}\mathcal{L}_C p.\end{aligned} \tag{II.7}$$

III. Robust GDAI Control Design

In this section, a tuning criterion is derived that ensures robust stability of the closed-loop MG dynamics (II.7) in the presence of clock drifts.

A. Error States and Problem Statement

We make the following standard assumption.

Assumption 3.1: The closed-loop system (II.7) possesses a synchronized motion. □

As the power flow equation (II.2) only depends on angle differences, following [26] we choose an arbitrary node, say node n and express all angles relative to that node, i.e.,

$$\theta = \mathcal{R}^\top \delta, \quad \theta \in \mathbb{R}^{n-1}, \quad \mathcal{R} = \begin{bmatrix} I_{n-1} \\ -\mathbb{1}_{n-1}^\top \end{bmatrix}.$$

Then, with Assumption 3.1, we introduce the error states

$$\begin{aligned}\tilde{\omega} &= \bar{\omega} - \bar{\omega}^* = \bar{\omega} - (I_n + \mu)^{-1}\mathbb{1}_n\omega^d,\\ \tilde{\theta} &= \theta - \theta^*, \quad \tilde{p} = p - p^*, \quad x = \text{col}\left(\tilde{\theta}, \tilde{\omega}, \tilde{p}\right).\end{aligned}$$

The resulting error dynamics of the system (II.7) is given by

$$\begin{aligned}\dot{\tilde{\theta}} &= \mathcal{R}^\top (I_n + \mu)^{-1}\tilde{\omega},\\ (I_n + \mu)M\dot{\tilde{\omega}} &= -D\tilde{\omega} - \mathcal{R}(\nabla U(\tilde{\theta} + \theta^*) - \nabla U(\theta^*)) + \tilde{p},\\ (I_n + \mu)\dot{\tilde{p}} &= (-\mathbf{B} + \mathbf{D}\mathcal{L}_C)\tilde{\omega} - \mathbf{D}\mathcal{L}_C\tilde{p},\end{aligned} \tag{III.1}$$

we define $x = \text{col}(\tilde{\theta}, \tilde{\omega}, \tilde{p}) \in \mathbb{R}^{3n-1}$ and $x^* = \mathbb{0}_{3n-1}$ is an equilibrium point of (III.1). Note that AS of $x^* = \mathbb{0}_{3n-1}$ implies AS of the synchronized motion from Definition 2.1 in system (II.7) up to a uniform shift of all angles [26]. As outlined in [10], [13] for the purpose of secondary frequency control, it is reasonable to assume that the clock drifts are bounded. This is formalized in the assumption below.

Assumption 3.2: $\|\mu\|_2 \leq \epsilon, \quad 0 \leq \epsilon < 1.$

We are interested in the following problem.

Problem 3.3: Consider the system (III.1) with Assumption 3.1. Determine the matrices $\mathbf{B}$, $\mathbf{D}$ and $\mathcal{L}_C$, such that AS of x^* is guaranteed for all μ satisfying Assumption 3.2.

B. Main result

For the presentation of our main result, it is convenient to define the matrices

$$\begin{aligned}T &= \begin{bmatrix} T_{11} & \frac{1}{2}\left(-I_n - \sigma\mathbf{D}^{-1}\mathbb{1}_n\mathbb{1}_n^\top D + \tilde{\mathbf{B}} - \mathcal{L}_\mathcal{C}\right) \\ * & T_{22} \end{bmatrix},\\ \hat{T}_2 &= \begin{bmatrix} \sigma M\mathbb{1}_n\mathbb{1}_n^\top\tilde{\mathbf{B}} & \sigma\mathbf{D}^{-1}\mathbb{1}_n\mathbb{1}_n^\top D \\ \mathbb{0}_{n\times n} & -\sigma\mathbf{D}^{-1}\mathbb{1}_n\mathbb{1}_n^\top \end{bmatrix},\end{aligned} \tag{III.2}$$

with $\sigma > 0$, $\tilde{\mathbf{B}} = \mathbf{D}^{-1}\mathbf{B} \geq 0$ and

$$\begin{aligned}T_{11} &= D - \frac{\sigma}{2}\left(M\mathbb{1}_n\mathbb{1}_n^\top\tilde{\mathbf{B}} + \tilde{\mathbf{B}}\mathbb{1}_n\mathbb{1}_n^\top M\right),\\ T_{22} &= \mathcal{L}_\mathcal{C} + \frac{\sigma}{2}\left(\mathbf{D}^{-1}\mathbb{1}_n\mathbb{1}_n^\top + \mathbb{1}_n\mathbb{1}_n^\top\mathbf{D}^{-1}\right).\end{aligned}$$

Furthermore, since μ is a diagonal matrix, with Assumption 3.2 we have that

$$\begin{aligned}\|\mu(I_n+\mu)^{-1}\|_2 &\le g_1(\epsilon), \quad g_1(\epsilon)=\tfrac{\epsilon}{1-\epsilon}>0,\\ \|(\mu^2+2\mu)(I_n+\mu)^{-2}\|_2 &\le g_2(\epsilon), \quad g_2(\epsilon)=\tfrac{\epsilon^2+2\epsilon}{(1-\epsilon)^2}>0.\end{aligned} \tag{III.3}$$

Our main result is as follows.

Proposition 3.4: Consider the system (III.1) with Assumption 3.1. Recall $g_1(\epsilon)$ and $g_2(\epsilon)$ defined in (III.3). Suppose that there exist $\sigma>0$, $\zeta>0$ such that

$$H_{\text{nom}}=\begin{bmatrix} M & -\sigma M\mathbb{1}_n\mathbb{1}_n^\top\mathbf{D}^{-1}\\ * & \mathbf{D}^{-1}\end{bmatrix} > \begin{bmatrix} g_2(\epsilon)M & \mathbb{0}_{n\times n}\\ \mathbb{0}_{n\times n} & g_1(\epsilon)\mathbf{D}^{-1}\end{bmatrix}, \tag{III.4}$$

and

$$\begin{aligned} T &> \left(\epsilon\zeta+g_1(\epsilon)\sqrt{\lambda_{\max}(D^2)+1}\right)I_{2n},\\ 0 &\ge \begin{bmatrix}-\zeta I_{2n} & \hat{T}_2\\ * & -\zeta I_{2n}\end{bmatrix},\end{aligned} \tag{III.5}$$

where T and $\hat{T}_2$ are defined in (III.2). Then, local AS of $x^*=\mathbb{0}_{3n-1}$ is guaranteed for all unknown clock drift factors satisfying Assumption 3.2.

Proof: Consider the Lyapunov function candidate

$$\begin{aligned} V=&\frac{1}{2}\tilde{\omega}^\top M\tilde{\omega}+U(\tilde{\theta}+\theta^*)-\nabla U(\theta^*)^\top\tilde{\theta}\\ &+\frac{1}{2}\tilde{p}^\top\mathbf{D}^{-1}(I_n+\mu)\tilde{p}\\ &-\sigma\tilde{p}^\top(I_n+\mu)\mathbf{D}^{-1}\mathbb{1}_n\mathbb{1}_n^\top M(I_n+\mu)\tilde{\omega},\end{aligned} \tag{III.6}$$

where $\sigma>0$ is a design parameter. The Lyapunov function V contains kinetic and potential energy terms $\tilde{\omega}^\top M\tilde{\omega}$, respectively $U(\tilde{\theta})$ [21], a quadratic term in secondary control input $\tilde{p}$ and a cross term between $\tilde{\omega}$ and $\tilde{p}$ which allows us to ensure that V is decreasing along the trajectories of (III.1).

First, we will show that V is indeed positive definite. Note that $\nabla_x V\big|_{x^*}=\mathbb{0}_{3n-1}$. This shows that x^* is a critical point of V. Moreover, the Hessian of V at x^* is given by

$$\nabla_x^2 V|_{x*}=\begin{bmatrix}\nabla^2U(\theta^*) & \mathbb{0}_{(n-1)\times n} & \mathbb{0}_{(n-1)\times n}\\ * & M & \nabla^2V|_{(2,3)}\\ * & * & \mathbf{D}^{-1}(I_n+\mu)\end{bmatrix}, \tag{III.7}$$

with $\nabla^2V|_{(2,3)}=-\sigma(I_n+\mu)M\mathbb{1}_n\mathbb{1}_n^\top\mathbf{D}^{-1}(I_n+\mu)$. Note that the matrix $\nabla^2U(\theta^*)>0$ [26]. Therefore, the Hessian $\nabla_x^2V|_{x*}$ is positive definite if and only if

$$\begin{bmatrix} M & -\sigma(I_n+\mu)M\mathbb{1}_n\mathbb{1}_n^\top\mathbf{D}^{-1}(I_n+\mu)\\ * & \mathbf{D}^{-1}(I_n+\mu)\end{bmatrix}>0. \tag{III.8}$$

By performing a congruence transformation using the positive definite matrix $S=\text{blkdiag}\left((I_n+\mu)^{-1},(I_n+\mu)^{-1}\right)$ and by invoking Sylvester's law of inertia [28], we see that the matrix on the left hand side of (III.8) is positive definite if and only if the following matrix inequality is satisfied

$$\begin{bmatrix}(I_n+\mu)^{-2}M & -\sigma M\mathbb{1}_n\mathbb{1}_n^\top\mathbf{D}^{-1}\\ * & (I_n+\mu)^{-1}\mathbf{D}^{-1}\end{bmatrix}>0. \tag{III.9}$$

The inequality (III.9) can be written as

$$H_{\text{nom}}-\begin{bmatrix}(\mu^2+2\mu)(I_n+\mu)^{-2}M & \mathbb{0}_{n\times n}\\ \mathbb{0}_{n\times n} & \mu(I_n+\mu)^{-1}\mathbf{D}^{-1}\end{bmatrix}>0,$$

where H_{nom} is defined in (III.4). Furthermore, since μ, M and $\mathbf{D}$ are all diagonal matrices, we have that

$$\begin{bmatrix}(\mu^2+2\mu)(I_n+\mu)^{-2}M & \mathbb{0}_{n\times n}\\ \mathbb{0}_{n\times n} & \mu(I_n+\mu)^{-1}\mathbf{D}^{-1}\end{bmatrix}\le\begin{bmatrix}g_2(\epsilon)M & \mathbb{0}_{n\times n}\\ \mathbb{0}_{n\times n} & g_1(\epsilon)\mathbf{D}^{-1}\end{bmatrix},$$

where $g_1(\epsilon)$ and $g_2(\epsilon)$ are defined in (III.3). Consequently, under the standing assumptions, see (III.4), $\nabla_x^2V|_{x*}>0$, confirming the positive definiteness of V. Note that $\nabla_xV\big|_{x^*}=\mathbb{0}_{3n-1}$ and $\nabla_x^2V|_{x*}>0$ implies that x^* is a strict local minimum of V [29].

Next, we calculate the time derivative of V along the solutions of (III.1), which yields

$$\begin{aligned}\dot{V}(\eta)=&-\tilde{\omega}^\top(I_n+\mu)^{-1}D\tilde{\omega}+\tilde{\omega}^\top(I_n+\mu)^{-1}\tilde{p}-\tilde{p}^\top\mathbf{D}^{-1}\mathbf{B}\tilde{\omega}\\ &+\sigma\tilde{p}^\top(I_n+\mu)\mathbf{D}^{-1}\mathbb{1}_n\mathbb{1}_n^\top D\tilde{\omega}-\sigma\tilde{p}^\top(I_n+\mu)\mathbf{D}^{-1}\mathbb{1}_n\mathbb{1}_n^\top\tilde{p}\\ &+\tilde{p}^\top\mathcal{L}_{\mathcal{C}}\tilde{\omega}-\tilde{p}^\top\mathcal{L}_{\mathcal{C}}\tilde{p}+\sigma\tilde{\omega}^\top(I_n+\mu)M\mathbb{1}_n\mathbb{1}_n^\top\mathbf{D}^{-1}\mathbf{B}\tilde{\omega},\\ =&-\eta^\top\begin{bmatrix}\mathbf{T}_{11} & \mathbf{T}_{12}\\ * & \mathbf{T}_{22}\end{bmatrix}\eta=-\eta^\top\mathbf{T}\eta,\end{aligned} \tag{III.10}$$

where $\eta=\text{col}(\tilde{\omega},\tilde{p})$ and

$$\begin{aligned}\mathbf{T}_{11}&=(I_n+\mu)^{-1}D\\ &\quad-\tfrac{\sigma}{2}\left((I_n+\mu)M\mathbb{1}_n\mathbb{1}_n^\top\mathbf{D}^{-1}\mathbf{B}+\mathbf{D}^{-1}\mathbf{B}\mathbb{1}_n\mathbb{1}_n^\top M(I_n+\mu)\right),\\ \mathbf{T}_{22}&=\mathcal{L}_{\mathcal{C}}+\tfrac{\sigma}{2}\left((I_n+\mu)\mathbf{D}^{-1}\mathbb{1}_n\mathbb{1}_n^\top+\mathbb{1}_n\mathbb{1}_n^\top\mathbf{D}^{-1}(I_n+\mu)\right),\\ \mathbf{T}_{12}&=\frac{1}{2}\left(-(I_n+\mu)^{-1}-\sigma(I_n+\mu)\mathbf{D}^{-1}\mathbb{1}_n\mathbb{1}_n^\top D+\mathbf{D}^{-1}\mathbf{B}-\mathcal{L}_{\mathcal{C}}\right).\end{aligned}$$

Note that the entries of the matrix $\mathbf{T}$ in (III.10) are uncertain, because the clock drift matrix μ is uncertain. Hence, to obtain verifiable conditions that ensure $\mathbf{T}>0$ and, thus, $\dot{V}(\eta)$ is negative definite, we note that $\mathbf{T}$ can be decomposed as

$$\mathbf{T}=T-\frac{1}{2}\left(\Gamma_1\hat{T}_1+\hat{T}_1^\top\Gamma_1\right)-\frac{1}{2}\left(\Gamma_2\hat{T}_2+\hat{T}_2^\top\Gamma_2\right), \tag{III.11}$$

where $\hat{T}_2$ is defined in (III.2) and

$$\begin{aligned}\Gamma_1&=\text{blkdiag}\left(\mu(I_n+\mu)^{-1},\mu(I_n+\mu)^{-1}\right),\\ \Gamma_2&=\text{blkdiag}\left(\mu,\mu\right),\quad \hat{T}_1=\begin{bmatrix}D & -I_n\\ \mathbb{0}_{n\times n} & \mathbb{0}_{n\times n}\end{bmatrix}.\end{aligned} \tag{III.12}$$

For any matrices $A\in\mathbb{R}^{n\times n}$ and $B\in\mathbb{R}^{n\times n}$, it holds that

$$AB+B^\top A^\top\le 2\|A\|_2\|B\|_2I_n.$$

Therefore from (III.11), we have that

$$\mathbf{T}\ge T-\left(\|\hat{T}_1\|_2\|\Gamma_1\|_2+\|\hat{T}_2\|_2\|\Gamma_2\|_2\right)I_{2n}.$$

Assumption 3.2 together with (III.3), implies that

$$\|\Gamma_1\|_2\le g_1(\epsilon),\quad \|\Gamma_2\|_2\le\epsilon,$$

where Γ_1 and Γ_2 are defined in (III.12). Therefore,

$$\mathbf{T}\ge T-\left(g_1(\epsilon)\|\hat{T}_1\|_2+\epsilon\|\hat{T}_2\|_2\right)I_{2n}. \tag{III.13}$$

From (III.12), we have that

$$\|\hat{T}_1\|_2=\sqrt{\lambda_{\max}(\hat{T}_1\hat{T}_1^\top)}=\sqrt{\lambda_{\max}(D^2)+1}.$$

Turning to $\hat{T}_2$,

$$\begin{aligned}&\|\hat{T}_2\|_2=\sqrt{\lambda_{\max}(\hat{T}_2\hat{T}_2^\top)}\le\zeta \quad\Leftrightarrow\quad \lambda_{\max}(\hat{T}_2\hat{T}_2^\top)\le\zeta^2,\\ \Leftrightarrow\quad &\hat{T}_2\hat{T}_2^\top\le\zeta^2I_{2n},\\ \Leftrightarrow\quad &\frac{1}{\zeta}\hat{T}_2\hat{T}_2^\top-\zeta I_{2n}\le 0,\end{aligned}$$

where $\zeta > 0$ is an upper bound for $\|\hat{T}_2\|_2$. By using the Schur complement [28], the last inequality above is equivalent to the second inequality in (III.5). Thus, from (III.13) we see that $\mathbf{T} > 0$ if

$$T - \left(\epsilon\zeta + g_1(\epsilon)\sqrt{\lambda_{\max}(D^2)+1}\right) I_{2n} > 0.$$

This is the first condition in (III.5). Thus, with the made assumptions, $\mathbf{T} > 0$ implies that

$$\begin{aligned} \dot{V}(\eta) &< 0 \quad \text{for} \quad \eta(t) \neq \mathbb{0}_{2n}, \\ \dot{V}(\eta) &= 0 \quad \text{for} \quad \eta(t) = \mathbb{0}_{2n}. \end{aligned} \tag{III.14}$$

This shows that x^* is stable. Recall $\eta(t) = \text{col}(\tilde{\omega}, \tilde{p})$ and therefore $\dot{V}(\eta)$ does not depend on $\tilde{\theta}$.

Therefore, to conclude local AS of x^*, we need to show that the following implication holds along solutions of the system (III.1)

$$\mathbf{T}\eta(t) \equiv \mathbb{0}_{2n} \quad \Rightarrow \quad \lim_{t\to\infty} x(t) = x^*. \tag{III.15}$$

Since $\mathbf{T} > 0$, from the second equation in (III.14), we have that $\tilde{\omega} = \mathbb{0}_n$ and $\tilde{p} = \mathbb{0}_n$, which, from (III.1), also implies that $\tilde{\theta}$ is constant. Moreover at $\eta(t) = \mathbb{0}_{2n}$, from the second equation in (III.1), we obtain that

$$\mathbb{0}_n = -\mathcal{R}(\nabla U(\tilde{\theta} + \theta^*) - \nabla U(\theta^*)),$$

which by multiplying from the left with $\mathcal{R}^\top$ and rearranging terms is equivalent to

$$\mathcal{R}^\top\mathcal{R}\nabla U(\tilde{\theta} + \theta^*) = \mathcal{R}^\top\mathcal{R}\nabla U(\theta^*). \tag{III.16}$$

Note that $\mathcal{R}^\top\mathcal{R}$ is invertible and recall that $\nabla^2 U(\theta^*) > 0$ [26]. Therefore, in a neighborhood of the origin, (III.16) only holds for $\tilde{\theta} = \mathbb{0}_{n-1}$. This shows that the implication (III.15) holds and hence ensuring AS of x^*, completing the proof. ■

Remark 3.5: By fixing the tuning parameter σ, the design conditions (III.4) and (III.5) are a set of LMIs that can be solved efficiently using standard software [30]. Furthermore, the design conditions are independent of an actual equilibrium point. Consequently, if they are satisfied, then the corresponding GDAI controller guarantees local AS of any synchronized motion of the closed-loop dynamics (III.1).

IV. Case study

In this section, the performance and robustness of a MG operated with the control (II.4) designed via the criterion (III.4),(III.5) is illustrated. At first, we introduce the employed MG and then the simulation scenario.

The MG (Figure 1) used in the case study is simulated using MATLAB®/Simulink® and PLECS [31]. Constant impedance loads are connected at all GFIs. The system parameters are given in Table I. In order to evaluate the robustness of (III.4),(III.5) with respect to further model uncertainties, a small positive line resistance value is considered in the simulations, see Table I. Based on [10], [11], [32], the clock drift factors for the simulated GFIs are chosen as $\mu_1 = 0$, $\mu_2 = 1\text{ms}$, $\mu_3 = 0.5\text{ms}$ and $\mu_4 = -1\text{ms}$. Thus, the clock of GFI1 in Figure 1 is chosen as the master clock and $\mathbf{B}$ is selected, such that $\mathbf{B}\mu = \mathbb{0}_{4\times 4}$ in (II.6). In the present

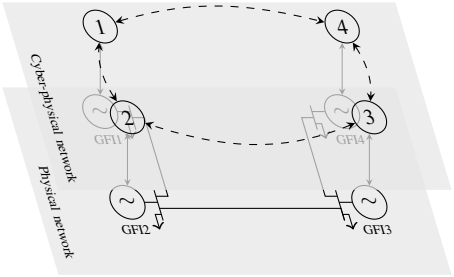

Fig. 1: MG used in simulation

TABLE I: MG parameters

Grid forming units		
Unit (at node)	M_i (MWs^2)	$D_i(MWs)$
GFI (1,2,3 and 4)	0.079	0.398
Constant impedance loads		
Unit (at node)	Apparent power [KVA]	Load power factor
Loads (1,2,3 and 4)	500	1
Line parameters		
Between nodes	Resistance [mΩ]	Inductance [μH]
1 and 2	0.71	20.2
2 and 3	3.5	101.2
3 and 4	2.8	80.9

case, this implies that $\mathbf{D}^{-1}\mathbf{B} = \tilde{\mathbf{B}} = \text{diag}(\tilde{b}, 0, 0, 0)$ where $\tilde{b} > 0$ is a design parameter. With the considered clock drift factors, $\epsilon = 0.001$ in Assumption 3.2.

The stability criterion (III.4), (III.5) is solved for $\mathbf{D}^{-1} > 0$, $\tilde{\mathbf{B}} \geq 0$ and $\mathcal{L}_\mathcal{C} \geq 0$ with $\sigma = 0.05$ and $\zeta = 2$ using the optimization toolbox Yalmip [30] and the solver Mosek [33] in MATLAB®/Simulink®. We obtained the control parameters

$$\mathbf{D} = \text{diag}(0.825, 1.174, 1.174, 1.174), \mathbf{B} = \text{diag}(2.578, 0, 0, 0),$$

$$\mathcal{L}_\mathcal{C} = \begin{bmatrix} 1 & -0.66 & 0 & -0.34 \\ -0.66 & 2 & -1.34 & 0 \\ 0 & -1.34 & 2 & -0.66 \\ -0.34 & 0 & -0.66 & 1 \end{bmatrix}.$$

The feasibility of (III.4), (III.5) implies that the equilibrium point of a GDAI controlled MG is locally asymptotically stable in the presence of clock drifts. Furthermore, we simulate the GDAI controlled MG shown in Figure 1 using the above-given control parameters. In simulation, PS weights [1], [26] were chosen as $\chi = D$ where $\mathcal{X} = \text{diag}(\mathcal{X}_i) \in \mathbb{R}^{n\times n}_{>0}$. The GDAI controller is activated at 10 seconds. In Figure 2, we can see that within a few seconds the *internal* inverter frequencies converge close to the nominal value ($\omega^d = 50\text{Hz}$), but not exatly to 50Hz in the presence of clock drifts. It has been shown in [1] that the aforementioned problem is noticeable even for usual distributed secondary frequency control schemes like [5], [6], [8], [9].

At first, we are interested in achieving $\omega^* = \omega^d$ using GDAI control (II.4), where ω^* is defined in (II.5). In the enlarged plot at 42.5 seconds in Figure 2, we can see that the synchronized electrical frequency ω^* (GFI1 frequency, green colored curve) coincides with $\omega^d = 50\text{Hz}$ and hence confirms that $\omega^* = \omega^d$ at steady state. Furthermore, between 0 to 10 seconds, the weighted power flows given by $(P_i - P_i^d)/\mathcal{X}_i, i \in \mathcal{N}$ do not reach consensus. At 10

seconds, when the GDAI controller is activated, the weighted power flows attain consensus at steady state, see the enlarged plot for weighted power flows at 42.5 seconds. At 50 and 75 seconds, a constant power load of $500\,\mathrm{kVA}$ with unity power factor is added at GFI4 and GFI3 respectively. The control performance following the additional load steps at 50, respectively, 75 seconds is also satisfactory.

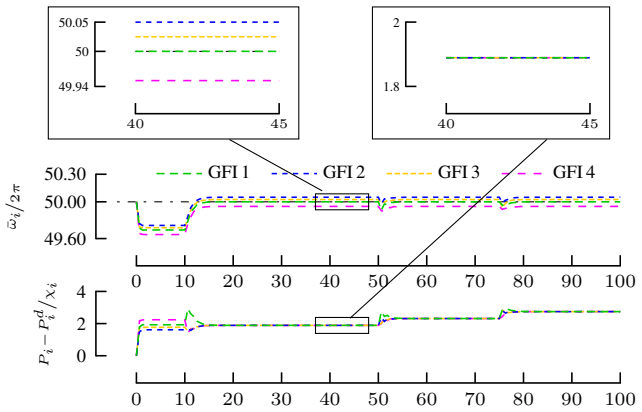

Fig. 2: Frequency ($\omega_i/2\pi$) and weighted power flows ($P_i - P_i^d)/\mathcal{X}_i$ versus time (in seconds)

V. Conclusions

A design criterion for a GDAI controlled MG ensuring robust stability in the presence of clock drifts is presented. Unlike existing solutions for secondary frequency control in MGs, GDAI control achieves accurate steady state frequency restoration, PS and local AS in the presence of clock drifts. Finally, numerical solution and simulated output confirms the accomplishment of the aforementioned control objectives.

Future research will incorporate time delays in communication network used in GDAI control. Also, we plan to test the GDAI controller on a real MG. Another interesting aspect is to consider time varying voltage amplitudes in the analysis.

Acknowledgment

J. Schiffer would like to thank K. Wulff for helpful comments and discussions on the proof of Proposition 3.4.

References

[1] A. Krishna, C. A. Hans, J. Schiffer, J. Raisch, and T. Kral, "Steady state evaluation of distributed secondary frequency control strategies for microgrids in the presence of clock drifts," in *25th Mediterranean Conference on Control and Automation (MED)*, 2017, pp. 508 – 515.

[2] J. Lopes, C. Moreira, and A. Madureira, "Defining control strategies for microgrids islanded operation," *IEEE Trans. Power Syst.*, vol. 21, no. 2, pp. 916 – 924, May 2006.

[3] J. Schiffer, D. Zonetti, R. Ortega, A. Stanković, J. Raisch, and T. Sezi, "Modeling of microgrids - from fundamental physics to phasors and voltage sources," *Automatica*, vol. 74, no. 12, pp. 135–150, 2016.

[4] J. Guerrero, P. Loh, M. Chandorkar, and T. Lee, "Advanced control architectures for intelligent microgrids – part I: Decentralized and hierarchical control," *IEEE Trans. Ind. Electron.*, vol. 60, no. 4, pp. 1254–1262, 2013.

[5] A. Bidram, F. Lewis, and A. Davoudi, "Distributed control systems for small-scale power networks: Using multiagent cooperative control theory," *IEEE Control Syst. Mag.*, vol. 34, no. 6, pp. 56–77, 2014.

[6] J. W. Simpson-Porco, Q. Shafiee, F. Dörfler, J. C. Vasquez, J. M. Guerrero, and F. Bullo, "Secondary frequency and voltage control of islanded microgrids via distributed averaging," *IEEE Trans. Ind. Electron.*, vol. 62, pp. 7025–7038, 2015.

[7] J. Schiffer, F. Dörfler, and E. Fridman, "Robustness of distributed averaging control in power systems: Time delays & dynamic communication topology," *Automatica*, vol. 80, pp. 261–271, 2017.

[8] X. Fu, F. Dörfler, and M. R. Jovanović, "Topology identification and design of distributed integral action in power networks," in *American Control Conference (ACC)*, 2016, pp. 5921 – 5926.

[9] C. D. Persis, N. Monshizadeh, J. Schiffer, and F. Dörfler, "A Lyapunov approach to control of microgrids with a network-preserved differential-algebraic model," in *CDC*, 2016, pp. 2595 – 2600.

[10] J. Schiffer, C. A. Hans, T. Kral, R. Ortega, and J. Raisch, "Modeling, analysis, and experimental validation of clock drift effects in low-inertia power systems," *IEEE Trans. Ind. Electron.*, vol. 64, pp. 5942 – 5951, 2017.

[11] Anritsu, "Understanding frequency accuracy in crystal controlled instruments - application note," Anritsu EMEA Ltd., Tech. Rep., 2001.

[12] N. M. Freris, S. R. Graham, and P. R. Kumar, "Fundamental limits on synchronizing clocks over networks," *IEEE Trans. Automat. Contr.*, vol. 56, no. 6, June 2011.

[13] J. Schiffer, R. Ortega, C. Hans, and J. Raisch, "Droop-controlled inverter-based microgrids are robust to clock drifts," *American Control Conference*, pp. 2341 – 2346, 2015.

[14] C. X. Rosero, H. Carrasco, M. Velasco, and P. Mart, "Impact of clock drifts on active power sharing and frequency regulation in distributed-averaging secondary control for islanded microgrids," in *International Autumn Meeting on Power, Electronics and Computing*, 2017.

[15] M. Castilla, A. Camacho, P. Martí, M. Velasco, and M. M. Ghahderijani, "Impact of clock drifts on communication-free secondary control schemes for inverter-based islanded microgrids," *IEEE Trans. Ind. Electron.*, 2017.

[16] J. T. Martínez, M. Castilla, J. Miret, M. M. Ghahderijani, and J. M. Rey, "Experimental study of clock drift impact over droop-free distributed control for industrial microgrids," in *43rd Annual Conference of the IEEE Industrial Electronics Society , IECON*, 2017.

[17] C. X. Rosero, P. Martí, M. Velasco, M. Castilla, J. Miret, and A. Camacho, "Consensus for active power sharing and frequency restoration in islanded microgrids subject to drifting clocks," in *IEEE 26th International Symposium on Industrial Electronics (ISIE)*, 2017.

[18] R. Solis, V. S. Borkar, and P. R. Kumar, "A new distributed time synchronization protocol for multihop wireless networks," in *CDC*, 2006, pp. 2734 – 2739.

[19] L. Schenato and F. Fiorentin, "Average timesynch: A consensus-based protocol for clock synchronization in wireless sensor networks," *Automatica*, vol. 47, no. 9, pp. 1878–1886, 2011.

[20] R. R. Kolluri, I. Mareels, T. Alpcan, M. Brazil, J. de Hoog, and D. A. Thomas, "Power sharing in angle droop controlled microgrids," *IEEE Trans. Power Syst.*, 2017.

[21] M. A. Pai, *Energy function analysis for power system stability*. Kluwer academic publishers, 1989.

[22] C. D. Persis and N. Monshizadeh, "Bregman storage functions for microgrid control," *IEEE Trans. Automat. Contr.*, 2017.

[23] C. Godsil and G. Royle, *Algebraic Graph Theory*. Springer, 2001.

[24] M. Mesbahi and M. Egerstedt, *Graph theoretic methods in multiagent networks*. Princeton University Press, 2010.

[25] P. Kundur, *Power system stability and control*. McGraw-Hill, 1994.

[26] J. Schiffer, R. Ortega, A. Astolfi, J. Raisch, and T. Sezi, "Conditions for stability of droop-controlled inverter-based microgrids," *Automatica*, vol. 50, no. 10, pp. 2457–2469, 2014.

[27] J. Schiffer, D. Goldin, J. Raisch, and T. Sezi, "Synchronization of droop-controlled microgrids with distributed rotational and electronic generation," in *CDC*, 2013, pp. 2334–2339.

[28] R. A. Horn and C. R. Johnson, *Matrix analysis*. Cambridge university press, 2012.

[29] A. van der Schaft, *L2-Gain and Passivity Techniques in Nonlinear Control*. Springer, 2000.

[30] J. Löfberg, "YALMIP : a toolbox for modeling and optimization in MATLAB," in *IEEE International Symposium on Computer Aided Control Systems Design*, sept. 2004, pp. 284 –289.

[31] Plexim GmbH, "Plecs software, www.plexim.com," 2013.

[32] *Schneider Electric, Conext XW inverter/charger product manual, 2014, [Online; accessed 8-November-2014]. [Online]. Available: http://www.schneider-electric.com/products/au*.

[33] Mosek, "The mosek optimization toolbox, www.mosek.com."